High Fidelity Methods and Physics for UAV Flow Regimes

Reid Melville, Miguel Visbal, and Raymond Gordnier
Air Force Research Laboratory, Air Vehicles Directorate (AFRL/VA), Computational Sciences Center, Wright-Patterson AFB, OH
{Reid.Melville, Miguel.Visbal, Raymond.Gordnier}@wpafb.af.mil

Abstract

Planned Air Force Unmanned Air Vehicles (UAVs) will be limited by highly nonlinear flow regimes, so an advanced simulation capability has been applied to this class of problems. The proposed paper will document several large-scale computational studies and efforts to validate and to extend the solver capability.

1. Introduction

Future planning studies for the DoD anticipate the adoption of UAVs as an integral part of the weapon system mix. Several UAV concepts are under consideration, and most of them represent revolutionary changes in planform and operations compared to legacy, manned systems. These new configurations and new operating conditions will reveal new limiting physics that will pose the challenge for future air operations. Some problems already identified included the vortex-induced pitch-up on some unmanned planforms, laminar-turbulent transition on high-aspect ratio ISR platforms, and installed engine performance for high altitude UAVs.

An advanced simulation capability was developed to address this class of problems. This numerical method utilized a centered compact finite-difference scheme to represent spatial derivatives that was used in conjunction with a low-pass Pade-type non-dispersive filter operator to maintain stability. A time-implicit approximately-factored matching algorithm was employed, and Newton-like subiterations were applied to achieve second-order temporal accuracy. Calculations were carried out on massively parallel computing platforms, using domain decomposition to distribute subzones on individual processors.

With the resources of this HPCMP DoD Challenge Project, this high-order solver was used both to validate and extend the capability and to research basic science issues related to UAV performance. Numerical investigations were made of scalability, grid sensitivity, and turbulence modeling effects. Also, a high-order overset grid capability was validated. The solver was used to assess the efficacy of flow control to improve turbine blade performance for high altitude UAVs. An investigation was made to document the effect of plunge motion on turbulent transition. Finally, an extensive research effort investigated the nonlinear aeroelastic response of Unmanned Combat Air Vehicles (UCAV)-style planforms under vortical buffet loads.

2. Solver Sensitivity Studies

Three different studies were conducted to better understand the performance and accuracy of the high-order, compact solver. First was a scalability study for the solver on the new, larger computers available at the MSRCs. Excellent scalability is sustained for up to 320 processors with the current version of the code as seen in Figure 1.

The next investigation was the continuation of numerical sensitivity studies on a large-eddy simulation (LES) of an airfoil at near stall conditions. This work consisted of parametric studies on grid topology, trailing edge geometry, use of sub-grid scale models, and angle-of-attack. All studies were accomplished with 12 million-point grids. Two major conclusions from the current and previous studies[1,2] are that spatial discretization had the primary influence on properly resolving flow structures and capturing transition. The high-order discretization displayed the ability to capture natural transition even on fairly coarse grids without special scheme modifications. Secondly, the implicit LES approach, which uses the compact solver and implicit filter of the scheme to dissipate energy instead of a sub-grid scale stress (SGS) model, gave almost identical results to the solver with a SGS model at half the computational cost.

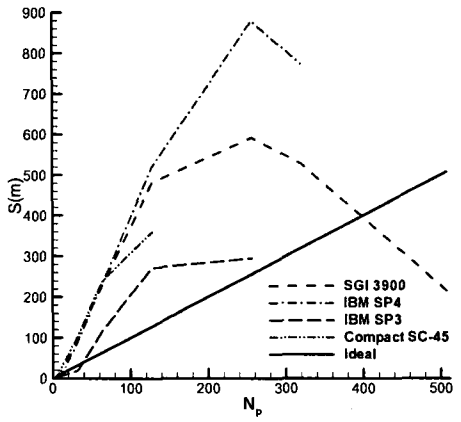

Figure 1. Speed-up of compact solver on available MSRC computers

The last study investigated the effects of varying methods of turbulence modeling for a simulation of flow control on a wall mounted hump. Comparisons were made on the hump between no flow control, constant suction, and oscillatory suction and blowing. This effort led to integration of a low-order k-epsilon model into the compact flow solver and subsequent development of a high-order k-epsilon model and a Reynolds Averaged Navier-Stokes (RANS)/ILES high-order hybrid model. Results were presented at the CFD Validation of Synthetic Jets and Turbulent Separation Control Workshop held at Williamsburg, VA, in March 2004. The most significant finding from this work includes solutions from high-order flow solvers that can be limited by use of a standard second-order turbulence model. Preliminary studies for this workshop demonstrated that either high-order discretizations or highly resolved meshes must be used for the turbulence models to recover the correct near wall behavior for a flat plate. This finding was reinforced in this study since the solutions for the high-order turbulence model matched the experimental data better than with a second-order model.

The above studies were critical in the development of tools to study, understand, and model separation and flow control for UAV wings.

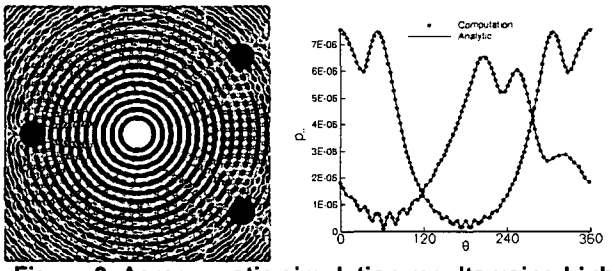

Figure 2. Aeroacoustic simulation results using high-order overset-grid algorithm

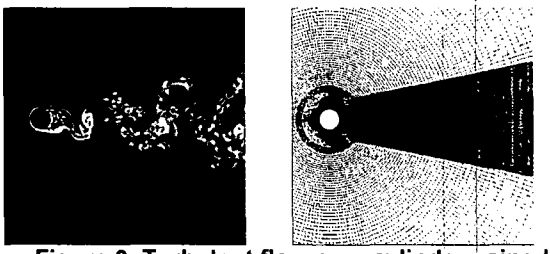

Figure 3. Turbulent flow over cylinder using high-order overset-grid algorithm

3. High-Order Overset Validation

High-order, compact algorithms used in the simulation of turbulence, aeroacoustics and electromagnetics have been shown to reduce the number of grid points and overall computational effort necessary to obtain solutions for a given accuracy. Through the application of overset grid techniques with high-order interpolation routines, these algorithms are now being employed on more complex geometries. Also, overset grid methods allow for additional grid resolution to be introduced locally in regions of high gradients, thus allowing for more effective utilization of existing resources. The development of this capability permits the application of powerful new computational tools to the prediction of aerodynamic performance and acoustic/electromagnetic signatures of complex UAV configurations.

To validate this new capability, various fundamental problems in aeroacoustics and turbulence have been investigated. Figure 2 shows the complex interference pattern generated by the scattering of sound waves generate from a time-dependent acoustic source by three circular cylinders. Also shown is the root-mean-squared pressure on the surfaces of the left and top-right cylinders obtained with this algorithm compared with existing analytic solutions. The high-order formulation matches extremely well, whereas the low-order formulation resulted in surface pressures that deviate noticeably from the analytic profile. Figure 3 shows the application of the method to turbulent flow over a cylinder at $Re_D = 3{,}900$. The use of a fine grid in the wake region produced similar results with three times fewer grid points compared to previous single-grid calculations.

Platforms used for these studies include the Compaq SC-40/45 and SGI 3900 parallel platforms at ASC MSRC. Number of processors utilized per run ranged from 20 to 64, and the run times ranged from 5–50 hours.

4. Separation Control on a Turbine Blade

One of the challenges arising in the use of UAVs for reconnaissance and combat missions is a loss of engine

performance when such platforms operate at low-Reynolds number conditions. Low-pressure turbines typically utilized by UAVs may encounter Reynolds numbers, based upon blade axial chord and inlet conditions, below 25,000 during high-altitude cruise. In such situations, boundary layers remain essentially laminar over a large portion of the turbine blades, even in the presence of elevated freestream turbulence levels. These laminar boundary layers are particularly susceptible to flow separation near the aft portion of a blade suction surface, resulting in a significant reduction in turbine efficiency, which may impose ceiling limitations for prolonged UAV operations.

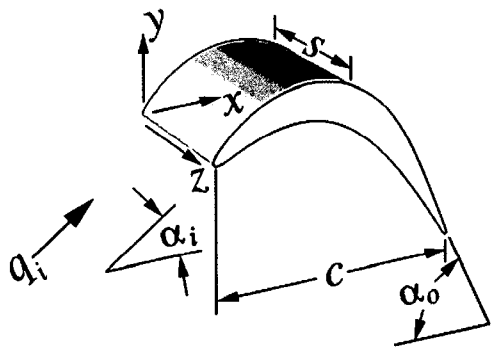

Figure 4. Schematic representation of the turbine blade configuration

Recent experiments have explored the feasibility of increasing the blade spacing at constant chord for low-pressure turbines, thereby raising the per blade loading. For practical applications, a higher loading can reduce the turbine part count and stage weight. Increased blade spacing however, is accompanied by increased boundary-layer separation on the suction surface of each blade due to uncovered turning, and results in reduced efficiency and wake losses. Vortex generator jets were then employed to mitigate these losses by maintaining attached boundary-layer flow over a greater distance along the blade surface.

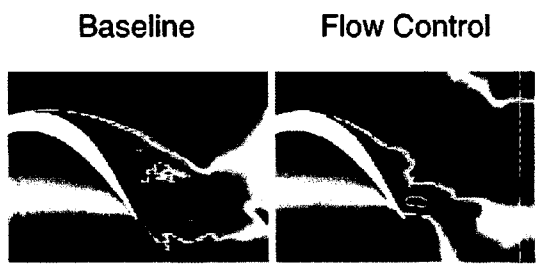

Figure 5. Instantaneous planar contours of the streamwise velocity component

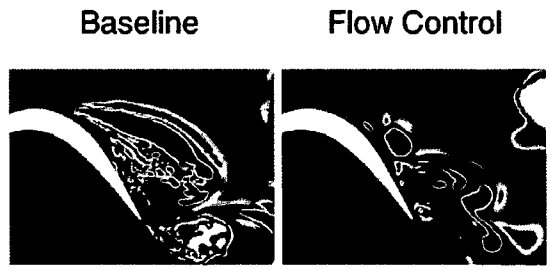

Figure 6. Instantaneous planar contours of the spanwise component of vorticity

The subsonic flow through a highly-loaded low-pressure turbine was simulated numerically using a high-order method. The configuration approximates cascade experiments that were conducted to investigate a reduction in turbine stage blade count, which can decrease both weight and mechanical complexity. At a nominal Reynolds number of 25,000, massive separation occurs on the suction surface of each blade. Pulsed injection vortex generator jets were then used to help mitigate separation, thereby reducing wake losses. Computations were performed for both uncontrolled and controlled cases, and reproduced the transitional flow occurring in the aft-blade and near-wake regions.

Features of the flowfields were elucidated, a grid resolution study was performed, and simulations were compared with each other, and with available experimental data. Relative to the uncontrolled case, it was found that pulsed injection maintained attached flow over an additional 15% of the blade chord, resulting in a 22% decrease in the wake total pressure loss coefficient.

Calculations were carried out on the NAVO MSRC IBM SP4. For the flow control case, approximately 18 million grid points were utilized, distributed over 275 processors. The simulation required 80,000 processing hours for the complete computation.

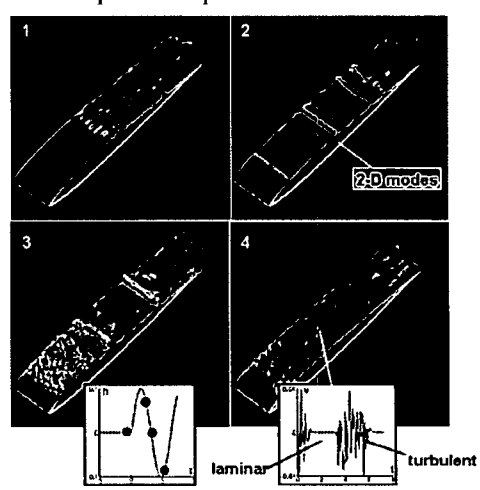

Figure 7. Time sequenced profiles of surface turbulence for a plunging NACA 0012, Re = 1.0 × 10^5, α= 5 °

5. Plunge-Induced Transition Dynamics

An exploratory computational study was performed for the dynamic simulation of transitional flow above a wing section undergoing a forced plunge maneuver. This scenario is of critical importance in UAV applications involving laminar flow control wherein off-design conditions, aero-elastic deformation or gust encounters may result in significant excursions in transition location. Variations in transition may in turn produce undesirable changes in aerodynamic performance, hysteretic effects in the aerodynamic loads, or even the aero-elastic coupling with the flexible vehicle structure. The initial results shown in Figure 7 demonstrate the dramatic excursions in transition location associated with the pitch-induced changes in effective angle of attack. Clearly seen in the picture is also the formation of spanwise-coherent vortical structures associated with flow re-laminarization and dynamic stall vortex formation. High-fidelity simulations may be used to guide and augment design tools for transition prediction.

6. Vortical Buffet for Elastic Planforms

UCAV configurations being developed need to be highly maneuverable while allowing for increased flexibility in the wing structure. Proposed vehicle designs incorporate low sweep (40 to 60 degrees) delta-type wing shapes. Extensive investigations of the unsteady, vortical flows that develop over highly-swept, (> 60 degrees) rigid delta wings at high angles of attack have been made both experimentally and computationally (see reviews by Visbal[7] and Rockwell[8]). Significantly less research has been undertaken for higher aspect-ratio delta wing configurations. Recent experimental measurements[9,10] and computations[11] for a 50° sweep rigid delta wing have shown distinct differences in the vortical flows that develop for this low sweep delta wing, both before and after the onset of vortex breakdown. These differences in the high angle of attack aerodynamics of the low sweep wing may also impact its dynamic structural response.

Experiments[12] for a highly flexible 50° sweep delta wing, Figure 8, exhibited sizable time-averaged deflections of the wing, Figure 9, and corresponding large amplitude vibrations in the post stall region, Figure 10. Accompanying this dynamic response was a switch in the dominant mode of vibration from the fundamental mode to the second antisymmetric mode. This aeroelastic behavior resulted in significant lift enhancement and a delay in stall, Figure 11.

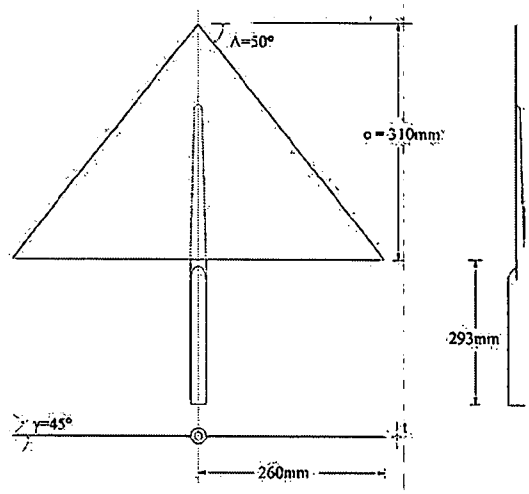

Figure 8. Delta Wing Geometry

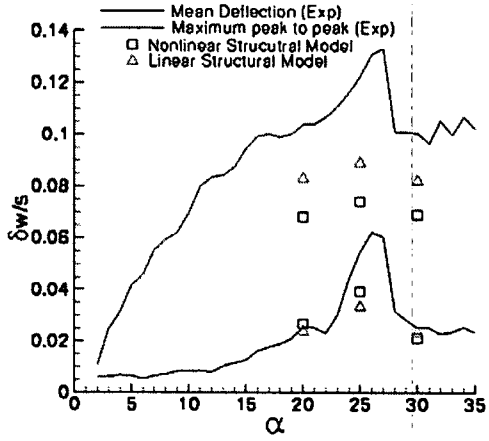

Figure 9. Variation with angle of attack of mean wingtip deflection and maximum peak to peak vibration amplitude normalized by semispan

A recent paper[13] by Gordnier and Visbal has investigated numerically the aeroelastic response of the same nonslender delta wing at high angles of attack. An aeroelastic code which couples an Euler solver with a finite element model for the von Karman plate equations is used for these computations. Implicit coupling of the aerodynamic and structural solvers is achieved via a subiteration strategy and the resulting scheme is second-order accurate in time. This code has been optimized for vector processing and has been implemented on the Cray SV1 using 4 nodes for multitasking. Computations were performed around the region of stall for angles of attack α=20°, 25°, and 30°.

For these calculations the flow and structural response were both assumed to be symmetric. The rapid increase in the rms acceleration of the wing tip was not evident in the computed results, Figure 10. Similarly,

while obtaining substantial delta wing deflections, Figure 9, and large amplitude vibrations, Figure 10, the numerical results did not capture the sharp increases in these quantities observed in the post stall region in the experiments. As a result no lift enhancement is obtained in this region, Figure 11. An increased influence of the 2nd symmetric mode was realized in the computations reminiscent of the switch in the dominant mode noted in the experiments. This increased influence of the 2nd structural mode was not seen when these computations were repeated using the linear structural model.

Analyzing the above results indicates that two separate issues need to be addressed to numerically capture the observed aeroelastic behavior for the delta wing. The first question is why the large increase in mean deflection and vibrations in the post stall region is not reproduced. The most likely reason for this is the assumption of symmetry in the present computations, which eliminates the influence of any antisymmetric modes. The experiments indicate, however, that the 2nd antisymmetric mode is excited in the post stall region leading to the increases in deflection and vibration amplitude. The second issue to be addressed is whether the inviscid Euler equations produce the proper vortical flow physics required to achieve the enhanced lift once the actual increase in the dynamic response is obtained. Future computations will address these issues by simulating the full delta wing geometry and by employing the fully viscous Navier-Stokes version of the aeroelastic code.

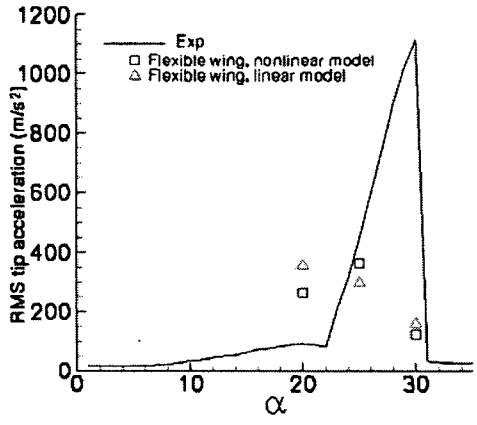

Figure 10. Variation of root mean square wingtip acceleration with angle of attack

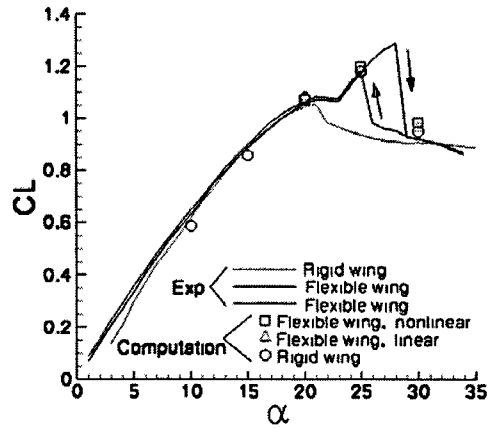

Figure 11. Variation of lift coefficient with angle of attack

7. Conclusion

A high-order compact solver was investigated, demonstrated, and applied on several challenging problems relevant to UAV applications. Assessments were made of the solvers numerical sensitivities and overset grid capability. Highly accurate, nonlinear simulations were performed and compared to better understand critical physics, such as separation, transition, and buffet. The research enabled by this HPCMP DoD Challenge Project has established the exceptional capabilities of this solver and begun the critical work of understanding the physics that dictate UAV performance.

References

1. Morgan, P. and M. Visbal, "Large-Eddy Simulation of Airfoil Flows." *AIAA Paper 2003-0777*, January 2003.

2. Morgan, P. and M. Visbal, "Large-Eddy Simulation Modeling Issues for Flow Around Wing Sections." *AIAA Paper 2003-4152,* June 2003.

3. Sherer, S., "Further Analysis of High-Order Overset Grid Method with Applications." *AIAA Paper 2003-3839*, Orlando, FL, June 2003.

4. Sherer, S., "Direct Numerical and Large-Eddy Simulations Using a High-Order Overset Grid Solver." *AIAA Paper 2004-2530*, Portland, OR, June 2004.

5. Rizzetta, D.P. and M.R. Visbal, "Numerical Investigation of Transitional Flow through a Low-Pressure Turbine Cascade." *AIAA Paper 2003-3587*, June 2003.

6. Rizzetta, D.P. and M.R. Visbal, "Numerical Simulation of Separation Control for a Transitional Highly-Loaded Low-Pressure Turbine." *AIAA Paper 2004-2204*, June 2004.

7. Visbal, M.R., "Computational and Physical Aspects of Vortex Breakdown on Delta Wings." *AIAA-95-0585*, January 1995.

8. Rockwell, D., "Three-Dimensional Flow Structure on Delta Wings at High Angle-of-Attack: Experimental Concepts and Issues." *AIAA-93-0550*, January 1993.

9. Ol, M.V. and M. Gharib, "The Passage Toward Stall of Nonslender Delta Wings at Low Reynolds Number." *AIAA-2001-2843*, June 2001.

10. Taylor, G.S., T. Schnorbus, and I. Gursul, "An Investigation of Vortex Flows over Low Sweep Delta Wings." *AIAA-2003-4021*, June 2003.

11. Gordnier, R.E. and M.R. Visbal, "Higher-Order Compact Difference Scheme Applied to the Simulation of a Low Sweep Delta Wing Flow." *AIAA-2003-0620*, January 2003.

12. Taylor, G.S. and I. Gursul, "Lift Enhancement over a Flexible Delta Wing." *AIAA-2004-2618*, June 2004.

13. Gordnier, R.E. and M.R. Visbal, "Numerical Simulation of Nonslender Delta Wing Buffet at High Angle-of-Attack." *AIAA-2004-2047*, April 2004.